Delineation of Cold-Prone Areas Using Nighttime SMS/GOES Thermal Data: Effects of Soils and Water[1]

E. CHEN, L. H. ALLEN, JR.[2], J. F. BARTHOLIC[3] AND J. F. GERBER

Fruit Crops Department and Agronomy Department, Institute of Food and Agricultural Sciences, University of Florida, Gainesville 32611

(Manuscript received 29 April 1981, in final form 19 April 1982)

ABSTRACT

Infrared digital data from geostationary satellites were used to demonstrate the usefulness of remotely sensed surface temperature data to delineate microscale and mesoscale climates. Nocturnal winter data (December–February) from 1976–77 to 1978–79 over Florida revealed noticeable contrasts in surface temperature patterns. Colder areas were associated with low soil moisture content in the upper layers of excessively-drained and well-drained sandy soils, whereas warmer areas were associated with bodies of water, wetlands, or poorly drained soils. An unexpected surface temperature pattern for one night where the north-central Florida climatic zone was colder than the north Florida climatic zone was found to be caused by differences in antecedent frontal rainfall. Differences in surface radiant energy fluxes over these two areas at 0200 EST 20 December 1977, based on average satellite-sensed surface temperatures, were compared with differences in soil heat fluxes that were computed from 1.5 m climatological temperatures and soil thermal properties by use of a simplified surface energy balance equation. The difference in computed soil heat fluxes was in reasonable agreement with the difference in radiant energy fluxes from the surface of the two areas. It was therefore concluded that this method could be used to compute differences in thermal inertia of the surface layer of different areas based on satellite and climatological temperature data.

1. Introduction

The upper soil layer, through radiant energy exchange, convective exchange with the atmosphere, and heat conduction to and from deeper soil layers, is one principal surface factor that influences microclimate (van Wijk, 1965). Surface temperatures vary in response to radiation exchange, soil heat flux, sensible heat flux, and latent heat flux of evapotranspiration and condensation. The volumetric heat capacity C and thermal conductivity λ of the upper soil layer are two soil properties that determine surface temperatures under given environmental conditions. The combination of these two properties, the thermal inertia $(\lambda C)^{1/2}$, governs the cyclic responses of surface temperatures and soil heat fluxes to daily and annual conditions. The water content strongly influences the heat storage capacity and the thermal conductivity of both organic and mineral soils (van Wijk, 1965). Because of variability of the properties of the surface soil layer (e.g., mineral and organic matter content, water content, texture, particle size and bulk density), the microclimate will vary from place to place. The difficulty of specifying soil properties such as thermal conductivity and heat capacity over a sufficiently large area makes it difficult to identify the magnitudes of dominant physical variables that cause observed microclimate variations.

Geiger (1965) provided some of the earliest detailed observations and causes of microclimates.The large diurnal temperature range of drained organic soils are known (Oliver, 1961), in contrast to the small diurnal range of wet peats (van Wijk, 1965). Vegetative cover modifies microclimate depending upon height and density (Allen *et al.*, 1972; Lemon, 1966; Glesinger, 1962). Because of low mass and rapid aerodynamic exchange of most vegetative cover compared with the surface layer of soil, vegetative cover microclimate effects are mediated primarily through changes in the height-distributed solar radiation absorption, and turbulent exchanges of sensible heat and latent heat (water vapor), rather than through thermal inertia. Therefore, heat storage changes in vegetation are usually ignored (Lemon, 1966) in energy balance studies.

To some degree, surface conditions, which help determine microclimate, can be manipulated to lessen climatic severity and provide some protection. The effect of water in microclimates can be illustrated

[1] Research supported in part by the Kennedy Space Center, National Aeronautics and Space Administration, Contract NAS10-8920. Florida Agricultural Experiment Stations Journal Series No. 2994.

[2] Supervisory Soil Scientist, USDA-ARS, and Assoc. Prof., Agronomy Department.

[3] Present affiliation: Assistant Dean for Research, Michigan State University.

0021-8952/82/101528-10$06.50

by the widely practiced method for frost and freeze protection through sprinkling and irrigation (Turrell, 1973), both to modify soil thermal properties and to ameliorate the microclimate directly. More recently, remote sensing technologies were applied to study soil moisture effects on microclimate (Schmugge, 1978; Chen *et al.*, 1979; Heilman and Moore, 1980) and lake effects on winter microclimate modification (Bill *et al.*, 1978). The study of the interaction of microscale and mesoscale climate has been hindered because of the lack of adequate data bridging those space scales. Earlier studies were generally confined to small areas with limited data points. To further study the contributing effects of surface and atmospheric parameters on microclimate, a system capable of providing continuous spatial and temporal information is needed.

Infrared digital data from the Synchronous Meteorological Satellite/Geostationary Operation Environmental Satellite (SMS/GOES) were used to provide surface temperature information to identify factors that generate differences in microclimates. These satellite data gave surface temperatures that represented the combined effect of all surface and atmospheric factors. Although the spatial resolution is not as fine as that obtained by polar-orbiting satellites (e.g., HCMM, TIROS, Landsat and NOAA Series), SMS/GOES does provide data every 30 min, rather than the much less frequent interval of polar-orbiting systems. Therefore, the time-series of weather and microclimate changes can be followed over diurnal cycles.

The first objective of this study was to show the capability of the low spatial resolution SMS/GOES data to delineate patterns of surface temperatures during winter nocturnal conditions. The second objective was to show associations between soil drainage classes and antecedent rainfall on the surface thermal patterns delineated from SMS/GOES data. The third objective was to test the hypothesis of antecedent rainfall effects on surface thermal inertia by comparing differences in nocturnal radiation with differences in calculated soil heat flux based on climatological (1.5 m) temperatures and literature-derived thermal inertias. A corollary to the third objective was to provide a method for computing thermal inertia differences of surfaces based on satellite and climatological temperature data.

2. Data

SMS/GOES nocturnal infrared (IR) digital data, obtained from the National Oceanic and Atmospheric Administration/National Meteorological Center (NOAA/NMC) were used in this study. The satellites were located at 35 800 km above the earth's equator at 75°W in geosynchronous orbit with the earth's rotation. GOES-1 was in stable orbit (1976–78) but was replaced by SMS-1 in January 1979 after the GOES-1 spin-scan became unreliable. Both satellites were equipped with an equivalent sensor system, the Visible and Infrared Spin-Scan Radiometer (VISSR) (Abbot, 1974). The sensor sweeps an entire earth frame in 18 min with 1821 north-south steps, and returns to the original position in 21 min ready to begin another sweep. The spin-scan series are initiated each 30 min. This nearly continuous data stream has a distinct advantage over polar-orbiting satellites for many types of climate research where sequential images over a diurnal cycle are needed. The VISSR IR (10.5–12.6 μm) data are digitized to 256 levels by NOAA/National Earth Satellite Service (NESS). Each count value corresponds to a temperature change of 0.5°C. Count values appropriate to Florida's nocturnal winter condition as calibrated by NOAA/NESS were supplied on request in a 129 × 129 pixel matrix. Data were requested by telephone from NOAA/NMC on mornings when the previous night was clear and while the data were still active in the disk file.[4] Some data were lost, due to human and weather factors, and data were not available during weekends and holidays.

The areal representation of each pixel was inferred from the digital maps by comparison with a physical map. Several determinations were made based on both north–south and east–west landmark features and an average scale value obtained. Each pixel in the digital map format was found to represent an area about 8 km (north–south) by 6 km (east–west) or ~48 km^2.

Data from a total of 9 (1976–77), 10 (1977–78) and 10 (1978–79) nights were obtained for the three winters. All of these nights occurred 1–2, and at most 3 days, after passage of cold fronts over the state. Clear skies and drier air masses were common behind the fronts. Atmospheric water vapor interference with surface emission is low under these conditions, but clouds occasionally interfered. The primary selection criterion for use of these data was that the sky over at least three-fourths of the state had to remain clear for 2–3 h before data were used. From a total of 29 nights, 7 nights were deleted due to cloud interference. Only 4 nights were usable from the available data of the 1978–79 winter.

The outline of Florida on the digital map was obtained by following a coastal isotherm determined from a sharp gradient in pixel temperature, aided by coastal city temperatures from NWS. At about one-third the distance down from the northern border of the state, enough latitudinal temperature change had occurred to usually require another isotherm (based on sharp changes in pixel temperatures) to be chosen

[4] Data are now archived by the Environmental Data and Information Service (EDIS), and are available at 30 min intervals.

to keep the coastal isotherms parallel to the physical coastline. The coastal isotherms chosen were ones that best followed the physiographic outline, but they do not necessarily represent the actual coastline. Chen (1979) gave details of this procedure.

All satellite digital images of the state were manually superimposed on a physical map of the same scale (Fig. 1) to avoid image errors introduced by orbit position variation of the satellite. Superposition was possible to ±1 pixel in south Florida. Radiance temperatures were checked against published climatological data (*Climatological Data*, 1977–79) over the entire state for gross inaccuracies. Radiance temperatures in central and southern Florida were compared with transect ground-truth temperatures collected for other concurrent research (Chen, 1979). The SMS/GOES surface temperatures showed a strong correlation with groundtruth (1.5 m) air temperatures, which confirms the strong influence from the surface. Radiance temperatures are integrated temperatures of surfaces of various compositions (e.g., vegetation, soil, water, or a combination of these). Problems introduced by atmospheric moisture were minimized by discussing only the difference in temperature patterns, as well as by selection of data from cold periods with dry air masses. The problem of low emissivity of silicious soils at wavelengths of 9.6 μm in the state were minimal because the area is almost wholly vegetated. Emissivities of agricultural and vegetated surfaces lie between 0.98 and 1.0 (Sutherland and Bartholic, 1977), corresponding to a temperature uncertainty of about 1°C, which is within the resolution of the VISSR sensor. Temperature patterns shown by SMS/GOES extended across various vegetative surfaces and hence across emissivity surfaces without any noticeable interruption. Therefore, temperature patterns are unlikely to be affected significantly by emissivities.[5]

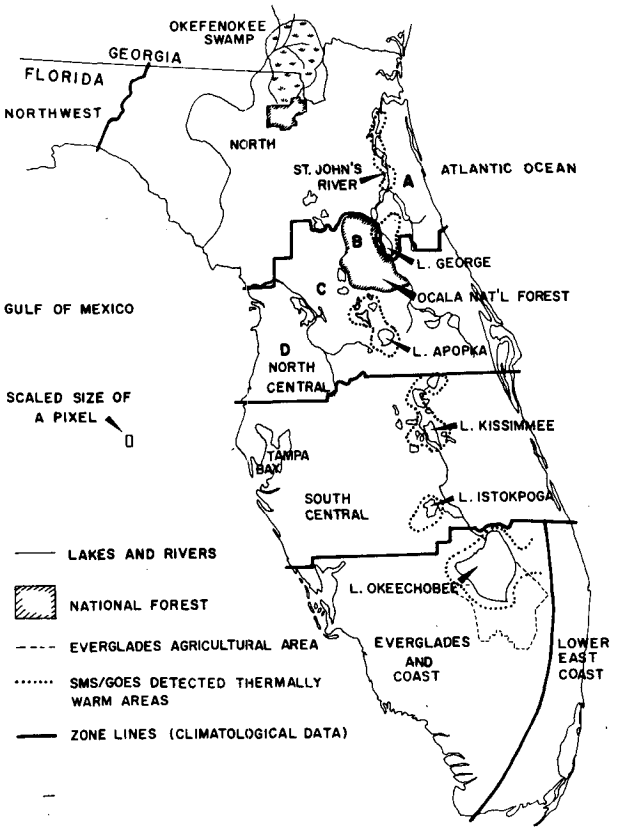

FIG. 1. Map of Florida showing the consistently warmer areas (dotted lines) detected by SMS/GOES during nocturnal winter conditions. Cold areas A, B, C and D are marked. Zone lines are as defined in *Climatological Data*, NOAA/EDIS, National Climate Center, Asheville, N.C.

3. Results

SMS/GOES surface digital IR data collected during clear nights after passage of cold fronts over Florida showed recognizable surface temperature patterns. These patterns remained relatively well-delineated throughout the three winters that were investigated. Data from 6 of 29 nights were selected to show early nighttime (1900–2200 EST) surface temperature patterns in Florida (Figs. 2a and 2b). Digital outlines of Lake Okeechobee showed the degree of superposition achieved in each map. Isotherm patterns illustrated large-scale atmospheric conditions and nocturnal cooling trends. Isotherms of 20 February 1977 (0°C) and 22 February 1978 (−2.2°C) showed typical Florida nocturnal winter conditions. The large temperature range (−8.2 to 6.8°C) of the isotherms in the three figures showed that these patterns were present under a wide range of atmospheric temperature conditions. Snow was recorded in north and central Florida on the afternoon of 19 January 1977, where the nocturnal isotherm was −8.2°C. The −2.2°C isotherm for 2300 EST 29 January 1978 was quite similar to an equivalent isotherm for 0400 and 0700 EST 15 January 1979 (Fig. 3).

One night (20 December 1977) of the SMS/GOES surface temperature data showed unusual temperature distributions in the Florida peninsula. A large area in north-central Florida was colder than all of north Florida, northwestern Florida, and part of Georgia (Fig. 4). The usual pattern for the previous night was shown in Fig. 2b (dotted line).

From the three thermal maps, prominent "cold-prone" areas in the state were noted and marked A, B, C and D. The colder area of the organic soil of the Everglades Agricultural Area was discussed in a previous paper (Chen *et al.*, 1979). Area A frequently

[5] Emissivity of surfaces across the 10.5–12.6 μm band of the IR radiometer is near 1.0, and avoids the problem of lower emissivities of silicious mineral soil surfaces at 9.6 μm. (Unpublished data of R. A. Sutherland.)

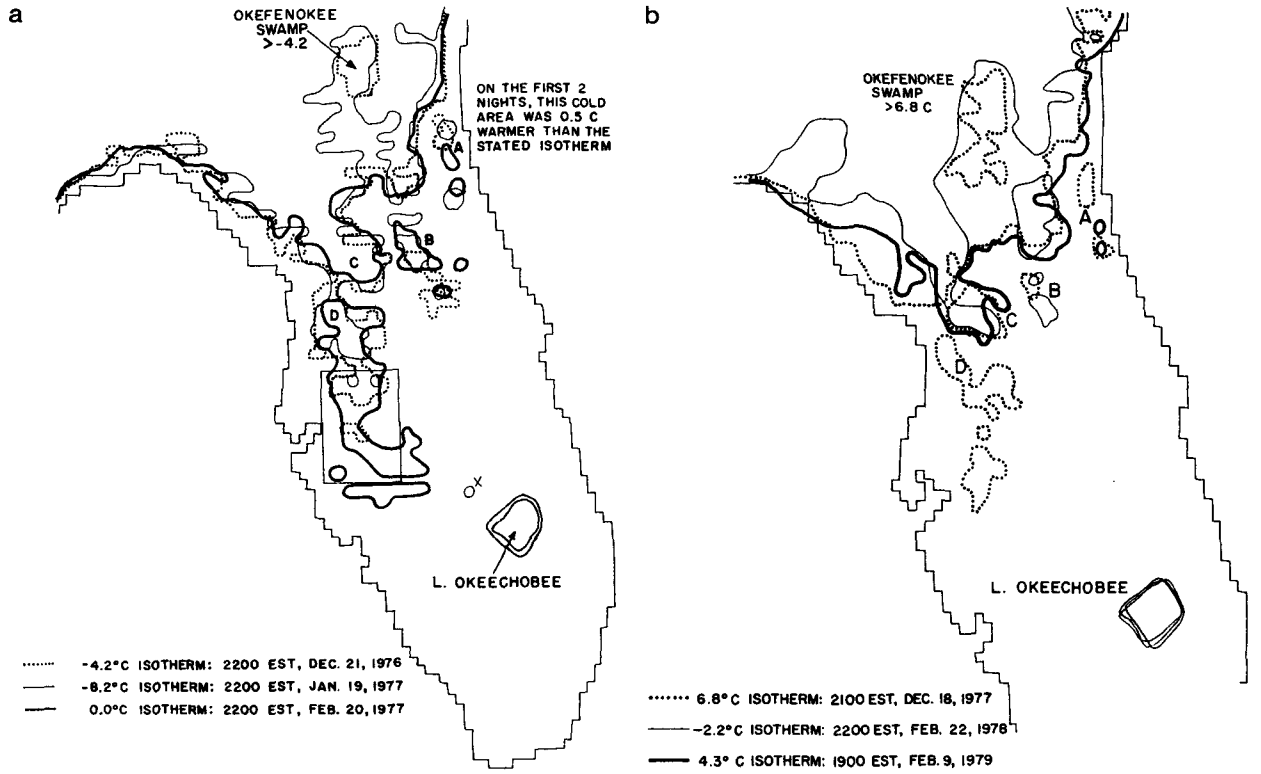

FIG. 2. Nocturnal surface thermal patterns for six Florida night-time conditions detected by SMS/GOES infrared sensors over the Florida Peninsula. Isotherms include all pixel temperatures equal to or less than the stated value. Lake Okeechobee is outlined to show the digital shape of the lake and the degree of accuracy achieved in the overlay. The boxed area shows a poorly defined but consistently colder area.

appeared as two to three small colder areas. Proximity to "warm" coastal water did not alleviate the lower temperatures detected by SMS/GOES. Area B is located within the geographical boundary of the Ocala National Forest. The forest consists of sparsely populated pine stands and is in the largest contiguous area of deep excessively-drained sandy soils in the Florida peninsula. The appearance of the coldest pixel in this area was found within 1 pixel of an elevated area (33–45 m vs 15 m for the general elevation of the forest). Cold areas C and D were found in areas of well-drained to moderately well-drained sandy soils. Infrequently, under very calm conditions, a single pixel was found northwest of Lake Okeechobee where it was generally colder than neighboring areas (Figs. 2a and 4, crosses). This pixel was within 1 pixel of excessively drained soils (Fig. 5, cross). The area is also the highest part of southern Florida (over 33 m) and constituted the southern terminus of the Central Florida Ridge Land Resource Area (Caldwell, 1980). The "ridge" is the highest part (33–45 m) of the central peninsula that includes the long finger of well-drained sandy soils that extend down the peninsula (Fig. 5). Thermal patterns also indicated that the western portion of south-central Florida was colder than the eastern portion of south-central Florida. LANDSAT imagery (e.g., the composite NASA ERTS-1 satellite image mosaic of Florida, 1973)[6] shows dendritic drainage patterns of streams in the western area, with less vegetative cover on the area as a whole, which indicates slightly better drainage. The eastern area shows more wetlands.

Several persistently warmer areas also showed up in the digital surface temperature maps. The most readily identifiable are the St. John's River between cold areas A and B, the lake area south of the Ocala National Forest, the Withlacoochee River basin between cold areas C and D and the Green Swamp area which is northeast of Tampa Bay and southeast of the cold area D (Fig. 1–4). Other data showed that lake-dominated areas of south Florida were also warmer (Fig. 1).

During winter nighttime conditions, the higher elevations in the state are frequently the colder areas because the soils are sandy and well-drained, whereas the lower elevations are frequently warmer areas because of the presence of wetlands or bodies of water (Fig. 5). However, the GOES IR pixel resolution is

[6] U.S. Geological Survey, EROS Data Center, Sioux Falls, SD 57198.

not fine enough to detect numerous small cold pockets of about 1 km^2 or less in area, that are found in dry karst[7] depressions, particularly in the "ridge" area of the state. Following a severe freeze on 12–13 January 1981, we observed extensive citrus tree damage in dry karst depressions, but less citrus tree damage than the surrounding area in karst depressions that contained a pond or lake at the bottom. The small-scale cold or warm pockets associated with elevation changes simply contribute to average pixel area temperatures. During cold winter events, we did not see any evidence of cold surfaces developing at lower elevations on the scale of the GOES IR pixel (6 × 8 km).

4. Discussion

The SMS/GOES thermal patterns (Figs. 2–4) remained sufficiently stable to be recognizable through three winters, which indicates strongly that specific surface properties must be responsible.

[7] An irregular limestone region with sinks and depressions.

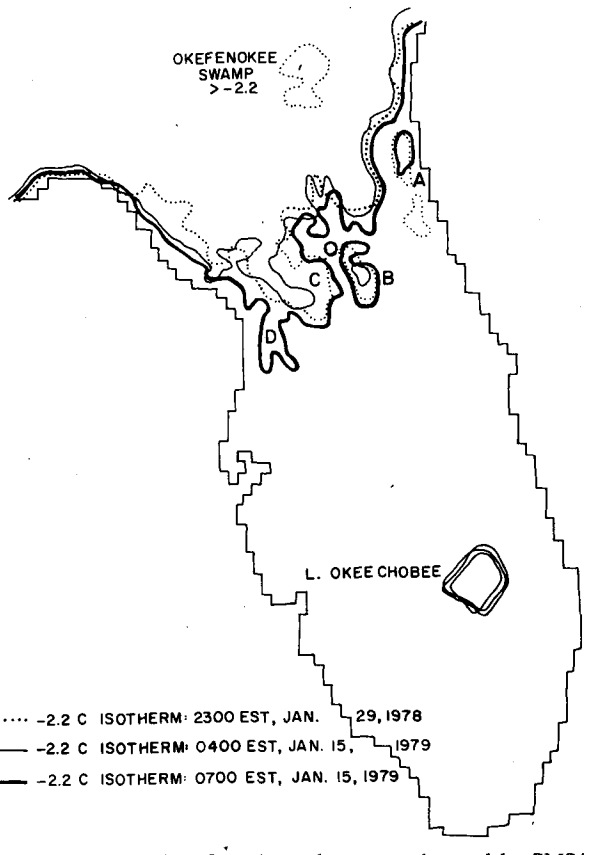

FIG. 3. Nocturnal surface thermal patterns detected by SMS/GOES comparing an early evening condition with early morning conditions one year later. Isotherms include all pixel temperatures less than or equal to the stated values. The thin and thick lines delineated the expansion of the cold area in a 3 h period on 15 January 1979.

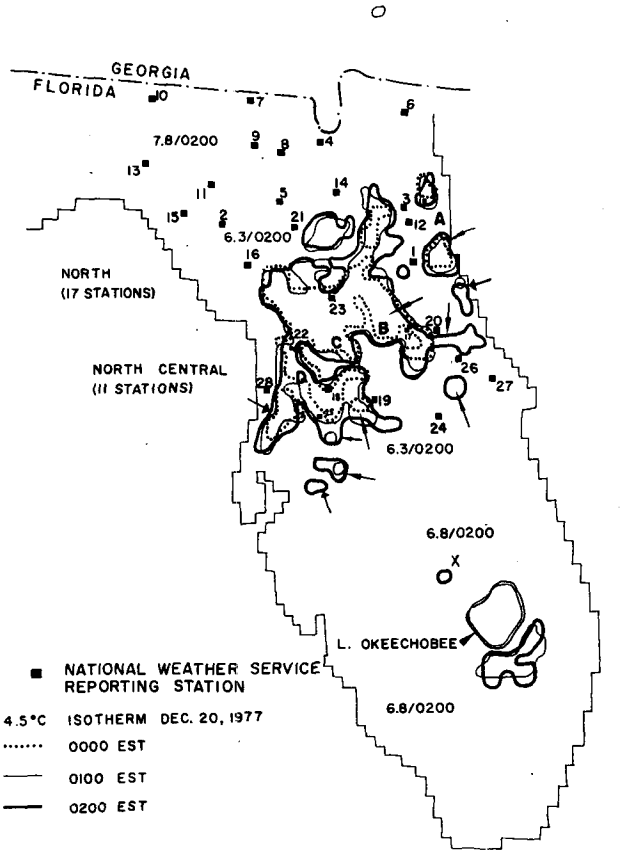

FIG. 4. Nocturnal surface temperature map of Florida from SMS/GOES data showing the large cold area in north-central Florida. Numbers indicate stations whose climate data were used in the test.

Higher temperature values were associated with water or wetland surfaces such as the St. John's River, the Okeefenokee Swamp and undrained Everglades, and the region of numerous small lakes throughout central Florida. These areas (Fig. 1, dotted lines) remained warmer than the surrounding areas throughout the nights examined.

The low temperature values from SMS/GOES corresponded to well-drained and excessively well-drained sandy soils where there was little or no surface water (Fig. 5). This pattern was especially true in the north, north-central and east-central Florida Peninsula, but it was not as evident in south-central Florida. The reason may be a combination of factors: the percentage of well-drained soils is less in south-central Florida, and there are many small lakes in the higher ridge area of the peninsula. The SMS/GOES thermal pattern of colder areas also corresponded closely to cleared areas suitable for row crops or pastures as shown by the composite 1973 NASA ERTS-1 satellite image mosaic of Florida and to three natural vegetation areas of Sand Pine-Scrub Forests, Longleaf Pine-Xerophytic Oaks and Hardwood Forests as clas-

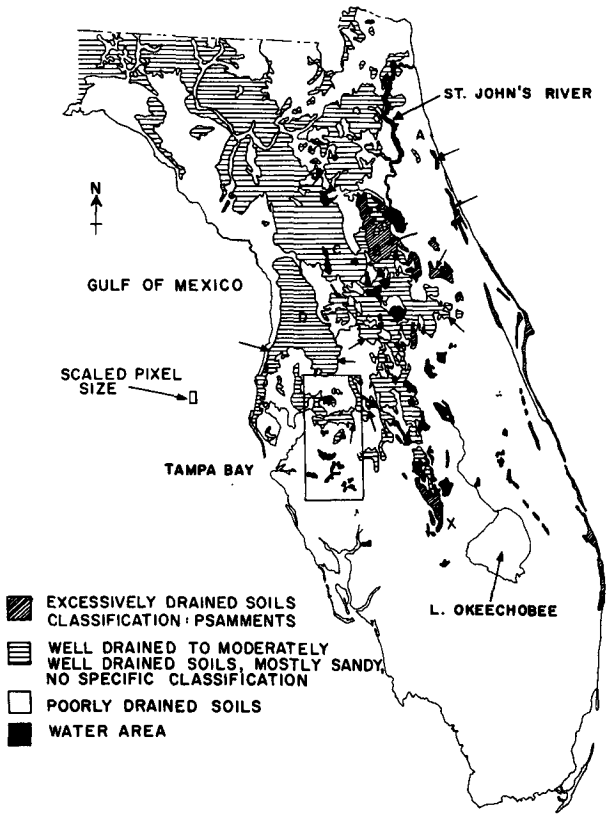

FIG. 5. Map of Florida showing soils drainage classes of sandy soils, from General Soil Map of Florida, Florida Agricultural Experiment Stations, Soil Conservation Service, 1962. Black areas are small lakes and the St. John's River.

sified by the General Map of Natural Vegetation in Florida (Davis, 1980). The patterns of satellite image and the vegetation map correspond very closely to the soils map of Fig. 5. Vegetation and land use are determined by soil conditions, rather than vice versa.

The Ocala National Forest (excessively drained sandy soil) and the Everglades Agricultural Area (drained organic soils) were also among the cold-prone areas. A common factor associated with cold patterns was the low surface soil moisture. In the first case, well-drained sandy soils that hold little moisture have low heat capacities, and in the second case, drained organic soils have not only low heat capacities, but also low thermal conductivities. The soil thermal effects override vegetation thermal effects during these nocturnal periods because of the mass of material. Vegetation maps and LANDSAT images show similar patterns as the Soils map (Fig. 5) mainly in response to soil water availability and suitability for agricultural development.

Florida sandy soils show an approximate 1.5-fold increase in soil moisture content from excessively-drained to well-drained classes, and from well-drained to poorly-drained classes. Within each soil drainage class, there is an approximate doubling of water content from the wilting point (15 bars) to field capacity (0.33 bar). Table 1 is a summary of Florida soil moisture characteristic data (Stewart *et al.*, 1963; Carlisle *et al.*, 1978). However, poor drainage characteristics of many of Florida's poorly-drained sandy soil classes are due more to a combination of low elevation and high water table, or to location in wetland sites, than to inherent physical properties. If the water table were lowered, such as in drainage for crop production, many of these soils would have the properties of well-drained sandy soils with natural deep water tables.

The influence of soil water in the upper layers on surface temperature is shown by the surface thermal patterns of 20 December 1977 (Fig. 4). A front passed through the state on the afternoon of 18 December. A "normal" cooling pattern was observed that night and delineated in Fig. 2b (dotted line, 6.8°C isotherm). On the following night, 19–20 December, the 4.5°C isotherm was used for each hour (Fig. 4) to show the unusual condition in which north-central

TABLE 1. Soil water contents (volume percent) and standard deviations at three water potentials of three soil drainage classes of sandy soils in Florida. Average values were derived from (A) Stewart *et al.* (1963) and (B) Carlisle *et al.* (1978). The values given were generally from the 0–20 cm layer. The number of samples averaged are shown in parentheses.

	Excessively drained sandy soils			Well drained sandy soils			Poorly drained sandy soils		
	Water potential (bars)			Water potential (bars)			Water potential (bars)		
Source	0.1[a]	0.33[b]	15.0[c]	0.1	0.33	15.0	0.1	0.33	15.0
A	5.0 (5)	—	2.2 (5)	11.5 (7)	—	4.6 (7)	19.3 (8)	—	9.6 (8)
B	8.3 (8)	4.8 (8)	2.0 (8)	11.1 (8)	7.7 (8)	3.4 (8)	14.8 (10)	9.91 (10)	4.0 (10)
	Standard deviation of the above samples of soil water content.								
A	1.5	—	0.3	4.2	—	1.3	12.1	—	5.3
B	3.7	1.4	0.8	3.3	1.7	1.0	3.7	2.7	1.0

[a] Limit to gravitational water.
[b] Field capacity.
[c] Limit to unavailable soil water, wilting coefficient.

Florida was colder than both north and northwest Florida. The small latitudinal temperature difference throughout the peninsula showed that the advective effect was minimal, and that the pattern was almost wholly due to surface radiation. The SMS/GOES data were consistent and repeatable at 0000, 0100 and 0200 EST. A reasonable explanation for the appearance of the cold area was the lack of frontal rainfall in north-central Florida. This explanation was supported by rainfall data (Table 2) on 16–18 December (*Climatological Data*, 1977). The main difference in rainfall between north and north-central Florida for the 3-day period occurred on 18 December, where an average of 18.4 and 0.96 cm of rain fell in north Florida and north-central Florida, respectively. The cold area was confined almost entirely to areas of well-drained soils in north-central Florida that received negligible rainfall. No other surface or atmospheric parameter except the difference in rainfall can account for this large abnormal thermal pattern, since the pattern extended across vegetative surfaces, and through the entire elevation across the peninsula.

The surface energy balance equation was applied to test the quantitative capability of SMS/GOES by using satellite temperature and average ground value temperatures. The areas tested were north (warm area) and north-central (cold area) Florida of 19–20 December 1977. Equations for the surface energy balance of the cold area, subscript c, and warmer northern area, subscript w, for nighttime situation were as follows:

$$(R\downarrow - R\uparrow)_c = (S + H + LE)_c\,, \qquad (1)$$

$$(R\downarrow - R\uparrow)_w = (S + H + LE)_w\,, \qquad (2)$$

where $R\downarrow$ is the longwave radiation from the sky and the atmosphere, $R\uparrow$ the surface radiation, S the soil heat flux, H the sensible heat flux and LE the latent heat flux. $R\downarrow$ can be assumed the same for both areas and may be ignored. H is proportional to $(T_{sfc} - T_{air})$, where T is temperature. However, under stable nocturnal conditions, H is small, because eddy diffusivity is relatively small. H (as well as LE) for the two areas are assumed to be the same because they are averages over large and relatively uniform surfaces having minimal topographic effect. The LE term at night is small because stomata of plants are closed and transpiration is near zero. Evaporation is much smaller than during the day because the main driving force, solar radiation, is not present. The other component of LE comes from the heat released on dew deposition. The latter will be approximately the same for both warm and cold areas since both areas are mostly vegetatively covered and the air mass behind a front is uniform. Therefore, assuming the $LE_c \approx LE_w$, and $H_c \approx H_w$, and taking the difference between Eqs. (1) and (2), we have the approximation,

$$R\uparrow_w - R\uparrow_c = S_c - S_w\,. \qquad (3)$$

TABLE 2. Climate data for the period 16–20 December 1977, showing average rainfall for north and north-central Florida for the 2 days before the passage of the front on 18 December and also on the 19th. The diurnal temperature range ($T_{max} - T_{min}$) for the 2 days after the passage of the front is shown. Data were generally taken at 0800 LT and were for the previous 24 h. Stations are identified by numbers and are shown in Fig. 4 (*Climatological Data*, 1977).

Stations North	24 h rainfall (cm)			$\Delta T = T_{max} - T_{min}$ (°C)		
	16	17	18	18	19	20
1 Crescent City	5.28	0.13	1.04	—	—	—
2 Cross City	*T*	*T*	1.12	11.1	17.8	19.4
3 Federal Point	6.02	0.08	1.14	8.3	15.0	16.1
4 Gainesville	1.04	*T*	1.75	8.3	20.0	18.4
5 Glen St. Mary	0.08	0.06	0.86	10.0	—	14.4
6 High Springs	0.03	*T*	2.39	10.0	20.1	17.2
7 Jacksonville	*T*	0.99	0.13	10.6	18.3	18.9
8 Jasper	—	—	0.94	13.3	17.8	20.6
9 Lake City	*T*	0.15	1.09	14.4	14.4	12.2
10 Live Oak	—	—	0.51	12.2	20.6	15.6
11 Madison	—	—	0.69	10.6	19.4	13.9
12 Mayo	—	1.19	—	12.2	17.2	18.3
13 Palatka	5.61	—	1.02	4.4	15.6	18.9
14 Perry	—	—	0.76	14.4	21.1	13.9
15 Stark	0.66	0.13	1.09	8.3	19.4	18.3
16 Steinhatchee	—	—	2.79	11.1	20.1	17.8
17 Usher Tower	0.71	—	1.12	7.2	21.1	18.3
Total rainfall	19.43	2.73	18.44	166.4	277.7	272.2
Average ΔT				10.4	18.5	17.0
Average T_{max}				22.2	21.3	21.6
Average T_{min}				11.1	2.8	4.6

Stations North-central	24 h rainfall (cm)			$\Delta T = T_{max} - T_{min}$ (°C)		
	16	17	18	18	19	20
18 Alexander Sp.	3.00	0.05	0.15	6.7	19.4	23.3
19 Bushnell	2.74	0.03	—	10.6	20.6	20.0
20 Clermont	1.70	—	—	6.1	13.9	17.2
21 Deland	0.89	0.15	—	—	21.1	23.3
22 Inverness	2.41	—	—	5.0	17.8	18.3
23 Ocala	1.14	0.05	—	6.7	20.6	25.0
24 Orlando	1.75	*T*	—	13.3	15.6	18.3
25 Saint Leo	2.57	—	—	5.6	15.0	20.6
26 Sanford	0.76	—	0.81	4.4	17.8	17.2
27 Titusville	0.69	1.50	—	5.6	17.2	17.2
28 WeekiWachee	0.79	0.05	—	8.3	16.1	18.9
Total rainfall	18.44	1.84	0.96	72.3	195.1	219.3
Average ΔT				7.2	17.7	19.9
Average T_{max}				22.8	22.2	23.1
Average T_{min}				15.2	4.5	3.2

An approximate solution of the soil temperature T at any cyclic time t and depth z (deVries, 1975) is

$$T(t, z) = T_a + \theta e^{-z/d} \cos(\omega t - z/d), \qquad (4)$$

where T_a, the average diurnal cyclic temperature, is constant, θ is the diurnal surface temperature ampli-

TABLE 3. Parameters used in the solution of Eq. (6).

Symbol	Parameter	Value
ϵ	Emissivity	0.98
σ	Stefan-Boltzmann's constant	56.7 nW $m^{-2}K^{-4}$
T_c	Average temperature of cold area (north-central)	277.0 K } average SMS/GOES pixel temperature
T_w	Average temperature of warm area (north Florida)	281.0 K } at 0200 EST, 20 December 1977
θ_c	Diurnal temperature amplitude of (cold area)	10.0 K } $(\Delta T)/2$, values obtained from Table 2
θ_w	Diurnal temperature amplitude of (warm area)	8.5 K }
$area_c$	Volume % water, well-drained soils, 15 bars, dry	3.4 } from Table 1
$area_w$	Volume % water, well-drained soils, .33 bar, wet	7.7 }
C_c	Volumetric heat capacity [a]	1.24 MJ m^{-3} K^{-1}
C_w	Volumetric heat capacity [a]	1.42 MJ m^{-3} K^{-1}
λ_c	Thermal conductivity [b]	0.50 W m^{-1} K^{-1}
λ_w	Thermal conductivity [b]	1.10 W m^{-1} K^{-1}
$(\lambda C)_c^{1/2}$	Thermal inertia (cold area)	0.79 kJ m^{-2} $s^{-1/2}$ K^{-1}
$(\lambda C)_w^{1/2}$	Thermal inertia (warm area)	1.25 kJ m^{-2} $s^{-1/2}$ K^{-1}
$\omega^{1/2}$	Frequency $(2\pi/86400)^{1/2}$	0.0085 $s^{-1/2}$

[a] C_c and C_w were obtained from an approximate equation from DeVries (1966): $C = x_s C_s + x_l C_l$, where x_s and x_l are volume fractions of solid material and liquid water, respectively. C_s and C_w are volumetric heat capacities of solid materal and water, respectively. $x_s = 0.55$, $C_s = 2.00$ MJ m^{-3} K^{-1} and $C_l = 4.19$ MJ m^{-3} K^{-1}.

[b] Values from deVries (1975).

tude, ω the frequency and d the damping depth, i.e., $d = (2\lambda/C\omega)^{1/2}$. The appropriate zero point for time is about 1400 local time when $T(0, 0)$ is at a maximum. Differentiating Eq. (4) with respect to z, and setting $z = 0$ at the surface, yields the surface soil heat flux,

$$S(t, 0) = -\lambda \frac{dT}{dz} = \theta(\lambda C)^{1/2}\omega^{1/2} \cos(\omega t + \pi/4). \quad (5)$$

The surface soil heat flux terms on the right-hand side of (3) were replaced by (5). The radiation terms on the left side were replaced by the Stefan-Boltzmann law, using average cold area and warm area surface temperatures obtained from satellite radiance temperatures. Eq. (3) then becomes

$$\epsilon\sigma(T_w^4 - T_c^4) = \{[\theta(\lambda C)^{1/2}]_c - [\theta(\lambda C)^{1/2}]_w\} \times \omega^{1/2} \cos(\omega t + \pi/4). \quad (6)$$

We chose to use the climatological average maximum and minimum temperatures at 1.5 m over the cold and warm areas to approximate the respective diurnal surface temperature amplitudes θ_c and θ_w (Table 3). First, vegetation temperatures over much of the area would not differ greatly from air temperature whether the vegetation is alive or senescent (Jackson *et al.*, 1981). Second, much of the area is covered in vegetation which intercepts and exchanges radiation so that actual soil surface temperatures would be near the vegetation temperature. Chen and Martsolf (1981) found a strong correlation of SMS/GOES surface temperature with 1.5 m air temperatures. Third, the surface soil of both areas would still be reasonably moist, although to a different extent between the cold and warm areas, so that daytime soil surface temperatures that drive soil heat flux would not be very different from air temperatures. Fourth, as discussed earlier, thermal inertia effects of the vegetation itself would be small compared to the soil.

We used soil thermal properties from deVries (1975) that are summarized in Table 3, and a sinusoidal approximation of the average diurnal cyclic temperature of the surface. Fourier series cannot be used because the ensemble of Fourier coefficients cannot be interpreted in terms of the soil thermal properties and a single harmonic of the diurnal cycle. Data of Kimball and Jackson (1979) showed that the temperature amplitude of the best fit natural harmonic would be about 85% of the temperature amplitude determined by one-half of the difference between maximum and minimum daily soil surface temperatures, and that the natural harmonic would account for about 86% of the variance of the observed soil surface temperature.

Because T_w and T_c were determined at 0200 local time, the appropriate t for use in Eq. (6) was 12 hours (or 43 200 seconds). Using values in Table 3, the two sides of Eq. (6) give

$$\epsilon\sigma(T_w^4 - T_c^4) = 19.3 \text{ W m}^{-2},$$

$$S(t, 0)_c - S(t, 0)_w = 16.4 \text{ W m}^{-2}.$$

Values of $(\lambda C)^{1/2}$ calculated from deVries (1975) and shown in Table 3 agree with the range of values from Geiger (1965) and Kimball and Jackson (1979).

Radiant energy differences obtained from satellite-derived radiance temperatures were reasonably similar to calculated soil heat flux differences obtained from averaged ground-level (1.5 m) diurnal temperature amplitudes (θ) and the calculated thermal in-

ertia of the soil surfaces. The agreement is good considering the approximate nature of available soil thermal property data and the approximations of the diurnal cyclic surface temperature.

The results were significant because they suggest a method to evaluate thermal inertia differences.Thermal inertia is important because it is the parameter governing the amplitude of heat flux which is directly related to soil thermal properties. The satellite temperature patterns (Fig. 4) show that thermal inertia is also an important parameter governing variations in mesoscale weather and climate of neighboring areas, and suggests that GOES IR temperatures can be used to delineate mesoscale climate.

The colder condition of the north-central Florida climatic zone detected by SMS/GOES was verified by the lower minimum temperatures recorded by the climatological data station. Averaged minimum temperatures for the north Florida zone and for the north-central Florida zone were 4.6 and 3.2°C, respectively, for 19–20 December 1977 (*Climatological Data*, December 1977). It was also reflected in the larger average diurnal temperature range (2θ) for north-central Florida zone (19.9°C) than for north Florida zone (17.0°C). However, without the satellite data, the correspondence of surface isotherms to soil drainage class would not have been identified. The hourly satellite data stream on 20 February helped trace the cooling pattern (Fig. 4) which showed little expansion of the cold area from 0000 to 0200 EST. Beyond the boundary indicated by the thermal pattern, further cooling was hindered by soil properties. During the previous day, both areas were clear and therefore received approximately the same amount of solar radiation. The small latitudinal temperature difference throughout the peninsula showed that advection was minimal and therefore the pattern was wholly due to surface radiation. Hence, it appears that satellite temperature maps may be used to detect surface effects that are distinguished from atmospheric advective effects.

This natural amelioration of nocturnal surface temperatures by antecedent rainfall implies that surface temperatures can be manipulated by application of water to alleviate cold temperatures. This may provide some degree of protection for crops under many conditions, especially where heaters or wind machines may be too costly or otherwise impractical.

Information obtained from the satellites cannot be supplied adequately by usual sources of air temperature data because 1) the small number of climate data points available does not give a spatial continuum, and 2) the surface may not be adequately characterized by 1.5 m air temperatures due to intermittent mixing and turbulence. On the other hand, surface temperatures from the satellite are unavailable during cloudy conditions, and atmospheric humidity causes interference. Due to low spatial resolution of the SMS/GOES thermal data, the temperature patterns delineated by SMS/GOES describe microclimate (i.e., the climate near the ground) on a mesoscale area rather than a micoscale area. However, the hourly data stream provided graphic information about the time-course of cold pattern development of surfaces which corresponded with surface thermal property conditions.

5. Conclusions

The SMS/GOES satellite data clearly revealed that, in Florida, surface conditions and soil properties are frequently the major factor causing neighboring areas to have different temperature regimes. Local conditions of the upper surface layers and transient atmospheric parameters such as rainfall frequently determine local mesoclimate. The colder areas detected by SMS/GOES were persistent throughout the three winters and were associated with excessively drained and well-drained sandy soil of low water-holding capacities, whereas the warmer areas were associated with surfaces with high moisture content. Results of heat flux and temperature modeling of the surface boundary layer (Carlson and Boland, 1978) showed similar relationships. Aircraft thermal data and the Heat Capacity Mapping Mission (HCMM) satellite data also indicate that the soil moisture content in the 0–4 cm soil layer is closely related to nocturnal temperature difference (Heilman and Moore, 1980). In our study, the satellite data for warm area and a cold area were evaluated quantitatively by using an approximate surface energy balance equation. Results showed good agreement between satellite surface temperature and ground-level thermal properties.

SMS/GOES thermal information can be used during clear sky conditions to detect climatologically different areas through thermal patterns and to explain the presence of these thermal patterns. Results can then be used to help produce more accurate local forecasts for freeze protection, and site selection (within the spatial resolution of the sensors) for reduced risks of cold damage.

The hourly data stream was effective in tracking the process of surface cooling. The repeatability of the surface temperature patterns, as shown from the hourly data stream, night-to-night comparisons and season-to-season persistence, added credence to the dependability and usefulness of remotely-sensed temperatures. Because of low spatial resolution, the data could delineate the ground-level climate patterns only on mesoscale areas. However, there is no network at ground level that can collect sufficient data to yield spatial temperature information equivalent to that of this satellite. Efforts should be continued to use these and other satellite data to gain more information on the effect of antecedent soil moisture conditions on thermal inertia and nocturnal minimum surface temperature patterns.

REFERENCES

Abbott, T. M., 1974: Visible infrared spin-scan radiometer (VISSR) for a synchronous meteorological spacecraft (SMS). Santa Barbara Research Center's VISSR Final Report, NASA, Goddard Space Flight Center, Contract NAS5-21139, Section 2.

Allen, L. H., Jr., E. Lemon and L. Muller, 1972: Environment of a Costa Rican forest. *Ecology,* **53,** 102–111.

Bill, R. G., Jr., R. A. Sutherland, J. F. Bartholic and E. Chen, 1978: Observations of the convective plume of a lake under cold-air advection conditions. *Bound.-Layer Meteor.*, **14,** 543–556.

Caldwell, R. E., 1980: Major land resource areas in Florida. *Soil Crop Sci. Soc. Florida Proc.* **39,** 38–40.

Carlisle, V. W., R. E. Caldwell, D. Sodec, III, L. C. Hammond, F. G. Calhoun, M. A. Granger and H. L. Breland, 1978: Characterization data for selected Florida soil. Soil Science Res. Rep. No. 78-1, USDA-Soil Conservation Service, 335 pp.

Carlson, T. N., and F. E. Boland, 1978: Analysis of urban-rural canopy using a surface heat flux/temperature model, *J. Appl. Meteor.*, **17,** 988–1013.

Chen, E., 1979: Estimating nocturnal surface temperature in Florida using thermal data from geostationary satellite data. Ph.D. dissertation, University of Florida, 280 pp.

——, and J. G. Martsolf, 1981: The development of nocturnal GOES infrared data as a source of climate information. Final Report, National Climate Program Office, NOAA, Contract NA80AA-D-00129, 174 pp.

——, L. H. Allen, Jr., R. G. Bill, Jr., J. F. Bartholic and R. A. Sutherland, 1979: Satellite-sensed winter nocturnal temperature patterns of the Everglades agricultural area. *J. Appl. Meteor.*, **18,** 992–1002.

Climatological Data, 1977–79: Climatological Data—Florida, 81–83. NOAA/EDIS/National Climatic Center, Asheville, NC.

Davis, J. G., 1980: General map of natural vegetation of Florida. Circ. S-178, Agricultural Experiment Stations, University of Florida.

deVries, D. A., 1966: Thermal properties of soils. *Physics of Plant Environment*, W. R. Van Wijk, Ed., North Holland Publ. Co., 210–235.

——, 1975: Heat transfer in soils. *Heat and Mass Transfer in the Biosphere*, Wiley, 5–28.

Geiger, R., 1965: *The Climate Near the Ground.* Harvard University Press, 611 pp.

Glesinger, E., Ed. 1962: *Forest Influences.* F.A.O., Rome, 307 pp.

Heilman, J. L., and D. G. Moore, 1980: Thermography for estimating near-surface soil moisture under developing crop canopies. *J. Appl. Meteor.*, **19,** 324–328.

Jackson, R. D., S. B. Idso, R. J. Reginato and P. J. Pinter, Jr., 1981: Canopy temperature as a crop water stress indicator. *Water Resour. Res.*, **17,** 1133–1138.

Kimball, B. A., and R. D. Jackson, 1979: Soil heat flux. *Modification of the Aerial Environment of Crops,* B. J. Barfield and J. F. Gerber, Eds., Amer. Soc. Agric. Eng., *Monog.*, No. 2, St. Joseph, MI, 211–229.

Lemon, E. R., 1966: Impact of the atmospheric environment of the integument of plants. *Proc. Fourth Int. Biometeorological Congress,* Rutgers University, New Brunswick, NJ, 57–69.

Oliver, J., 1961: Soil temperatures in an upland peat bog. Memorandum No. 4, Report on the Fourth Symposium on Agricultural Meteorology, Aberystwyth.

Schmugge, T., 1978: Remote sensing of surface soil moisture. *J. Appl. Meteor.*, **17,** 1549–1557.

Stewart E. H., D. P. Powell and L. C. Hammond, 1963: Moisture characteristics of some representative soils of Florida. ARS 41-63, Agricultural Research Service and Soil Conservation Service, USDA, 53 pp.

Sutherland, R. A., and J. F. Bartholic, 1977: Significance of vegetation in interpreting thermal radiation from a terrestrial surface. *J. Appl. Meteor.*, **16,** 759–763.

Turrell, F. M., 1973: The science and technology of frost protection. *The Citrus Industry*, Vol. 3, University of California, Division of Agricultural Science, 110 pp.

van Wijk, W. R., 1965: Soil microclimate, its creation, observation and modification. *Meteor. Monog.*, No. 28, Amer. Meteor. Soc., 59–73.